ACS APPLIED MATERIALS & INTERFACES

Research Article

Cite This: ACS Appl. Mater. Interfaces 2018, 10, 23399−23405

www.acsami.org

Achieving Higher Strength and Sensitivity toward UV Light in Multifunctional Composites by Controlling the Thickness of Nanolayer on the Surface of Glass Fiber

Chao Sun,[†] Jie Zhang,*[,†] Shang-Lin Gao,[‡] Nan Zhang,[†] Yi-Jun Zhang,[†] Jian Zhuang,[†] Ming Liu,[†] Xiao-Hui Zhang,[§] Wei Ren,*[,†] Hua Wu,[∥] and Zuo-Guang Ye*[,⊥]

[†]Electronic Materials Research Laboratory, Key Laboratory of the Ministry of Education & International Center for Dielectric Research, School of Electronic and Information Engineering, Xi'an Jiaotong University, Xi'an 710049, China

[‡]Leibniz-Institut für Polymerforschung Dresden e.V. Hohe Strasse 6, 01069 Dresden, Germany

[§]MOE Key Laboratory of Biomedical Information Engineering, School of Life Science and Technology, Xi'an Jiaotong University, Xi'an, 710049, China

[∥]Department of Applied Physics, Donghua University, Songjiang, 201620 Shanghai China

[⊥]Department of Chemistry and 4D LABORATORIES, Simon Fraser University, Burnaby, British Columbia V5A 1S6, Canada

Supporting Information

ABSTRACT: The interphase between fiber and matrix plays an essential role in the performance of composites. Therefore, the ability to design or modify the interphase is a key technology needed to manufacture stronger and smarter composite. Recently, depositing nanomaterials onto the surface of the fiber has become a promising approach to optimize the interphase and composites. But, the modified composites have not reached the highest strength yet, because the determining parameters, such as thickness of the nanolayer, are hardly controlled by the mentioned methods in reported works. Here, we deposit conformal ZnO nanolayer with various thicknesses onto the surfaces of glass fibers via the atomic layer deposition (ALD) method and a tremendous enhancement of interfacial shear strength of composites is achieved. Importantly, a critical thickness of ZnO nanolayer is obtained for the first time, giving rise to a maximal relative enhancement in the interfacial strength, which is more than 200% of the control fiber. In addition, the single modified fiber exhibits a potential application as a flexible, transparent, in situ UV detector in composites. And, we find the UV-sensitivity also shows a strong correlation with the thickness of ZnO. To reveal the dependence of UV-sensitivity on thickness, a depletion thickness is estimated by a proposed model which is an essential guide to design the detectors with higher sensitivity. Consequently, such precise tailoring of the interphase offers an advanced way to improve and to flexibly control various macroscopic properties of multifunctional composites of the next generation.

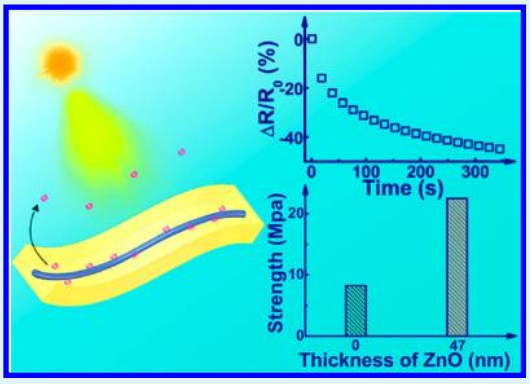

KEYWORDS: *ZnO nanolayer, multifunctional composites, interfacial strength, atomic layer deposition, UV detector*

1. INTRODUCTION

Gaining a higher mechanical strength has always been a challenging goal in the design and fabrication of fiber reinforced composites (FRC), which have been one of the most widely used materials due to their high stiffness to weight ratio, excellent durability, and design flexibility.[1] It has been well-known, an effective approach to enhance the strength of FRC is the modification of the interphase between fiber and polymer matrix, which plays an important role in determining the physical properties of composites. Thus, various treatments on the surfaces of the fiber, including chemical[2−4] and physical[5,6] (heat and plasma) methods, have been carried out to optimize the interfacial properties. Recently, depositing nanomaterials onto the surfaces of fibers has been regarded as a promising method to obtain higher quality FRC. Sager et al. achieved an improvement of 71%[7] in interfacial shear strength (IFSS) of carbon fiber-modified epoxy composites when carbon nanotubes (CNTs) were grown onto the surfaces of fibers by a chemical vapor deposition (CVD) process. However, the high temperature and chemical atmosphere during the CVD growth process reduced the tensile strength of the fiber by 30%. To avoid the degradation of the fiber, some low-temperature methods (≤200 °C), such as electrophoretic deposition[8,9] and hydrothermal process,[10−13] have been

Received: March 26, 2018
Accepted: June 18, 2018
Published: June 18, 2018

DOI: 10.1021/acsami.8b04872
ACS Appl. Mater. Interfaces 2018, 10, 23399−23405

adopted to deposit the nanolayers onto the fibers and realized a great improvement (30−110%) in the IFSS. However, these mentioned methods can hardly control the distribution and thickness of the nanolayer, which should be an important parameter determining the mechanical property of interphase and composite. Therefore, the question still remains open: what is the critical thickness of nanolayer on the surface of fibers that would lead to an optimized enhancement of IFSS?

Besides the enhancement of IFSS by the in situ modification on fibers, various nanomaterials are expected to introduce new functions into the traditional composites.[8,14−16] Among them, the nanoscale ZnO materials, such as quantum dots, nanowires, and nanorods, have drawn much attention because of their potential for broad applications in piezoelectric devices, gas sensors, transparent electrodes, etc.[17,18] But, to date there have been few reports on the relationship between the thickness of ZnO nanolayer (or film) and the environmental response, for example, the UV-sensitivity. In fact, an optimized thickness can not only improve the properties of the device but also achieve environmental friendliness, especially by reducing the extra energy consumption.

In this work, to address above open questions associated with the relationship between the thickness of nanolayer and the macroscopic performances of composites, the atomic layer deposition (ALD) approach was exploited to deposit ZnO onto the glass fiber because of its relatively low deposition temperature and its ability to precisely control the deposition thickness at nanoscale. At the same time, ALD technology can achieve a uniform and conformal 3D deposition onto the curved surfaces of glass fiber.[19] The dependence of the interfacial strength of the composites on the thickness of coated ZnO nanolayer is studied by the fragmentation test, and importantly, a critical thickness corresponding to the highest improvement of the relative IFSS has been found for the first time. Moreover, the modified fiber by ZnO not only dramatically enhances the interfacial strength, but also shows a high sensitivity toward UV light as a minitype sensor. By introducing a depletion thickness, a model is proposed to explain the process of sensing UV light and predict the sensitivity of single fiber detector correlated to the thickness of ZnO nanolayer. So our investigations provide an insight into the designing of multifunctional composites materials with high strength and sensitivity by precisely controlling the thickness of nanolayer.

2. EXPERIMENTAL METHODS

2.1. ZnO Nanolayer Growth. ZnO nanolayers were deposited onto glass fiber at 200 °C by ALD (Picosun R200, Finland) process, during which Diethylzinc (DEZ 99.9999%, Suzhou Fornano Electronic Technology Co., Ltd., China) and deionized water were used as precursors for zinc and oxygen, respectively. The precursors first reacted with the surface chemical species for nucleation and then formed ZnO layer by layer via alternatively introducing different precursors to the Reactor Chamber.[20] ZnO nanolayers with various thicknesses, from 21 to 75 nm, were precisely controlled by the number of ALD cycles. The alkali-resistant glass fibers with an average diameter of 15 μm (Leibniz-Institutfür Polymer forschung Dresden, German), were used as control fiber.

2.2. Fiber/Epoxy Composites Preparation. Single glass fibers were mounted within a dog-bone shaped silicone rubber mold. Epoxy resin (Epoxy 618, Shanghai Resin Factory co., Ltd., China) and hardener (H-7020, ShenzhenYexu Industry co., Ltd., China) with a weight ratio of 100:32 were thoroughly mixed and degassed prior to pouring into the mold. The fiber/epoxy composites were then cured at 80 °C for 12 h, and the dimensions of specimens for fragmentation tests were: 20 mm for gauge length, 3.5 mm for width and 2.6 mm for thickness. Table 1 includes the important symbols in this work.

Table 1. Symbols and Parameters Related to the Equations in the Paper

symbol	definition
τ	interfacial shear strength
σ_f	critical tensile strength of glass fiber
l_c	critical length of fiber fragment
E_f	elastic modulus of the fiber
E_m	elastic modulus of the matrix
t_{ZnO}	thickness of ZnO nanolayer
$t_{depletion}$	initial depletion thickness on ZnO nanolayer
$t'_{depletion}$	decreased depletion thickness under UV light

2.3. Characterization Method. The SEM and EDS images were taken on FEI Quanta FEG 250 (U.S.A.) and MERLIN Compact (German), respectively. The XRD patterns were obtained on a Rigaku D/Max-2400 diffractometer (Japan).

2.4. Single Fiber Fragmentation Test. The specimens were measured by using a FM-12 tensile test (Beijing Fuyouma Technology Co., Ltd., China) equipment at room temperature, at a 0.0005 mm/s stretch rate. Meanwhile, a polarized light microscopy system was used to in situ monitor the process and to observe the birefringent patterns of fiber fragmentation within the epoxy matrix.

2.5. Single Fiber Tensile Strength Measurement. Single fiber was stretched by a Model YG (B) 006 electronic single yarn strength tester (Changchun kexin Co. China) at room temperature. Three different gauge lengths including 5, 10, and 15 mm are chosen for the tensile strength measurement. The stretch rate is 10 mm/min. Utilizing the extrapolation, the tensile strength of single fiber at critical length was obtained (the detailed content is shown in Supporting Information (SI).)

2.6. Resistance Measurement under UV Light. The DC resistance of the modified fiber was recorded under ultraviolet irradiation. The fiber was connected to two Au electrodes via silver paste on glass substrates, and the modified fiber segment (~0.8 cm) served as the gauge length of the sample. For the sensitivity test of the single fiber composites under UV light, a fiber was embedded into transparent epoxy. A spectrofluorometer (Quanta Master TM40) provided static UV light and the wavelength of the specific UV light was 379 nm. Simultaneously, a DC digital multimeter (Keithley 2002) was used to record the change of resistance through a 2-wire model.

3. RESULTS AND DISCUSSION

3.1. Structural Characterization of ZnO Nanolayer on the Fiber. Figure 1a,b shows the scanning electron microscopy (SEM) images of a glass fiber coated with 75 nm thick ZnO, which display an uniform morphology and randomly orientated ZnO grains on the fiber surface. An energy-dispersive X-ray spectroscopy (EDS) mapping of the fiber surface shown in Figure 1c, indicates that the whole fiber has been homogeneously covered by ZnO according to the distribution of Zn element (purple). The X-ray diffraction (XRD) pattern reveals a polycrystalline hexagonal wurtzite structure of ZnO layer (Figure 1d). The uneven background of the XRD pattern is caused by the glass substrate.

3.2. Thicknesses of ZnO Nanolayer on the Fiber. ZnO nanolayers are deposited onto the surfaces of glass fibers by the ALD technique. The thickness of ZnO can be precisely controlled by changing the cycle number, because the reaction on the surface is self-limiting during the ALD process,[20] The deposited thickness dependent on the cycle number is shown in Figure 2. The inserted SEM images indicate a linear relationship between the thickness of ZnO nanolayer and the

DOI: 10.1021/acsami.8b04872
ACS Appl. Mater. Interfaces 2018, 10, 23399−23405

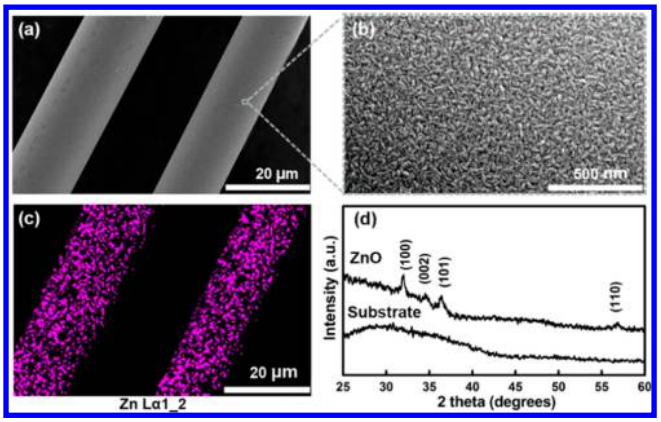

Figure 1. (a) Scanning electron microscope image of the ZnO nanolayer deposited on the surface of glass fibers by ALD. (b) An enlarged surface morphology of the ZnO nanolayer. (c) Energy dispersive spectroscopy of the ZnO nanolayer on the surface of the glass fibers. (d) X-ray diffraction patterns of the as-deposited ZnO and the glass substrate background.

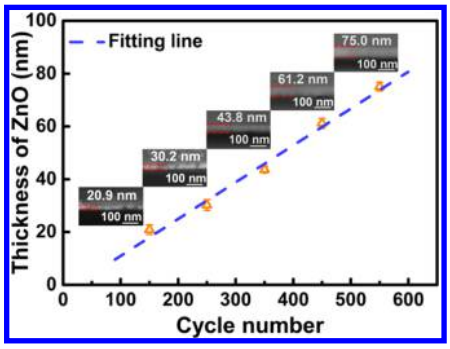

Figure 2. Dependence of the ZnO thickness on the number of depositing cycle. The blue dash line is a linear fitting for the growth rate of ZnO nanolayer (r^2 = 0.984). The inserted SEM images are the cross sections of ZnO nanolayers on the glass fiber with different growth cycles: 150, 250, 350, 450, and 550, respectively.

growth cycles. Based on the fitted result, the growth rate of ZnO nanolayer is about 1.4 Å/cycle.

3.3. Fragmentation Test of Single Fiber Composites.

In order to investigate the influence of the ZnO nanolayer thickness on the IFSS, the fragmentation test on single fiber composites was carried out, which is widely used to estimate the performance of interphase in FRC. A single fiber is planted into a dog-bone shaped polymer matrix, and then a tensile load is applied on the sample by stretching the two sides along the length direction of the fiber. With increasing strain, the fiber keeps fracturing until the fragments become too short to build up a sufficiently high tensile load. According to the constant shear model proposed by Kelly and Tyson,[21] the interfacial shear strength (τ) can be calculated from

$$\tau = \frac{\sigma_f}{2\left(\frac{l_c}{d}\right)} \quad (1)$$

where σ_f is the critical tensile strength of the fiber, d refers to the diameter of the fiber in the composites, l_c is the critical length which is obtained by multiplying the experimental mean fragment length with a factor of 4/3.[22] The ratio (l_c/d) refers to the critical aspect ratio, which is an inverse measure of the interfacial shear strength. First, by polarized light microscope measurement, the birefringent patterns in Figure 3a show that the increased number of fragments in the modified FRC, which indicates a stronger interphase produced by the introduction of the ZnO nanolayer. Based on the measured critical aspect ratio (Supporting Information (SI) Figure S1) and the critical tensile strength (SI Figure S2, S3), the IFSS values for the fibers treated by ZnO nanolayer with different thickness are calculated according to eq 1 and shown in Figure 3b. Obviously, the IFSS of all of the ZnO-modified fiber composites is enhanced compared with the control fiber group. In particular, the sample coated with 44 nm ZnO layer achieves a maximal IFSS, that is, about 200% over that of the control group. Notably, it is also the highest relative enhancement among the already published results. The enhancement obtained in our work is nearly twice as high as the result (113%)[10] reported in ZnO nanowire-modified carbon fiber composites and much higher than the other nanomaterials-modified fiber composites, such as CNT-modified FRC (~90%).[23] The two main reasons that contribute to this tremendous improvement of IFSS during the ALD process includes (i) the homogeneous distribution of ZnO can effectively 'heal' the surface defects and flaws of glass fibers[24] and prevent the fragments arising from stress under a tensile load; (ii) the effect of mechanical interlock between the fiber and the epoxy is enhanced by the ZnO nanograins.

From the mechanics point of view, the IFSS is affected by the local modulus of the interphase according to the stress transfer models in single fiber composites proposed by Galiotis et al.[25] and Asloun et al.[26] From the stress transfer models, the critical aspect ratio can be expressed as

$$\frac{l_c}{d} = \alpha k_0 \left(\frac{E_f}{E_m}\right)^{1/2} \quad (2)$$

where α has two discrete values corresponding to thermosetting or thermoplastic polymers and elastomers, k_0 is a theoretical constant related to the material. E_f and E_m refer to the elastic modulus of the fiber and matrix around the interphase, respectively. Additionally, according to the rule of mixture,[1] the longitudinal modulus of the matrix around the coated fiber, $E_{m'}$, can be calculated:

$$E_{m'} = E_{ZnO} \cdot V_{ZnO} + E_m \cdot (1 - V_{ZnO}) > E_m \quad (3)$$

where, E_{ZnO} and E_m represent the elastic modulus of ZnO film and epoxy, respectively, and V_{ZnO} is the volume fraction of the ZnO nanolayer distributed in the interphase formed within a short-range of epoxy matrix. Due to the much higher elastic modulus of ZnO thin film (61−168 GPa)[27,28] than that of epoxy (~3 GPa),[29] the modulus of polymer around interphase is increased to E_m', and the critical aspect ratio is consequently decreased. Higher modulus of the interphase helps prevent the propagation of cracks. Therefore, it is clear that the high modulus of ZnO nanolayer helps to improve the strength of the interphase based on eqs 1−3.

Furthermore, according to the results shown in Figure 3b, we observe a novel dependence of the IFSS of composites on the thickness of the modified-ZnO. With the increase of the thickness of ZnO nanolayer, the IFSS gradually increases to its maximum until the nanolayer reaches 44 nm in thickness. This is because the interphase modified by ZnO prevents the debonding and the propagation of cracks between fiber and matrix, as shown Figure 3c I and II, respectively. When the thickness exceeds 44 nm, the IFSS shows a little decrease instead of further enhancement with the increasing thicknesses.

DOI: 10.1021/acsami.8b04872
ACS Appl. Mater. Interfaces 2018, 10, 23399−23405

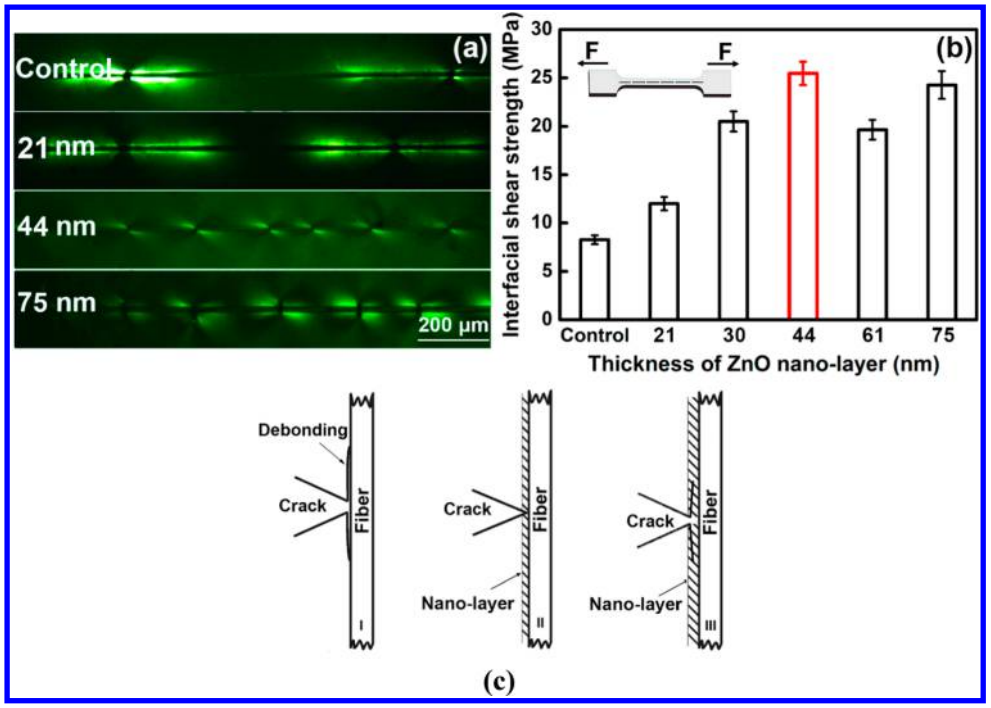

Figure 3. (a) The birefringent patterns under polarized light microscope during the fragmentation test. (b) The calculated interfacial shear strengths of the control group and groups modified by ZnO with different thicknesses according to eq 1. The error bars represent standard errors. (c) A model reveals the crack process changes with an increase of nanolayer thickness in fiber reinforced composites.

It may be due to the restriction of resin impregnation of fibers by the thicker ZnO layer, resulting in defects in final composites and the fracture mode transferring from radial segmentation in the coating to an axial debonding at the ends of the coating (see Figure 3c III).[30] Based on above results, we find a critical thickness corresponding to the highest interfacial strength, which is 44 nm in our case. Below this thickness, the number of debonding patterns is decreased with the increased nanolayer. While the thickness exceeds the critical value, the other debonding mode may occur in the coating layer that does not cause further improvement in the interfacial strength. Therefore, the thickness of modifying nanolayer plays a significant role in determining the IFSS of the composites. A proper thickness is needed not only to form a stronger composite but also to save extra energy consumption. Therefore, the critical thickness can be regarded as a reference value for fabricating the significantly stronger and tougher composites.

3.4. Photoconductive Properties of Single ZnO-Coated Glass Fiber. In addition to enhance the mechanical strength in FRC, ZnO nanolayer is expected to introduce various sensing functions to the insulating glass fiber, due to the unique electric and optical properties of ZnO. By comparing with the other ZnO based devices,[17] the single fiber modified by ZnO is smaller in size and more suitable for flexible device. Especially, combined with polymer matrix, the modified fiber can be used in some specific environment. Here, we attempt to use a single fiber coated by ZnO as an in situ UV detector, due to its wide bandgap of the as-deposited ZnO which is simulated to be 3.24 eV from the Tauc plot (SI Figure S4).

To confirm this application as an in situ UV detector, the single modified fibers were embedded into the epoxy matrix, Figure 4a schematically shows the test process of the single fiber used as a UV detector. The DC resistance of the fiber

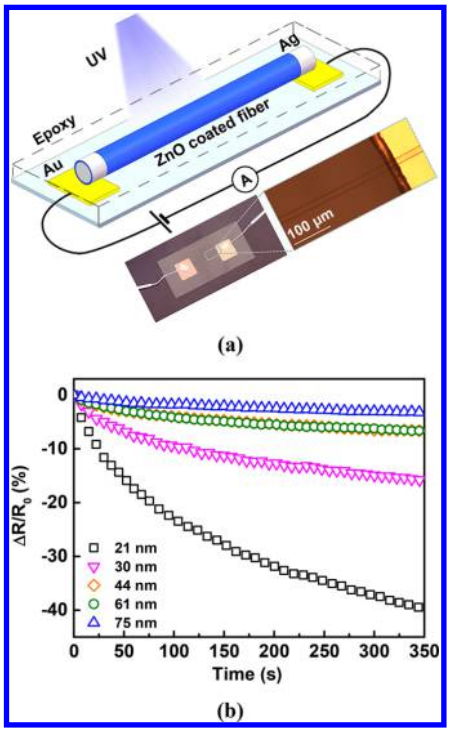

Figure 4. (a) Schematic illustration showing the test process of a single fiber as a UV-detector under UV light. The bottom optical images are the single fiber between two Au electrodes. (b) Time dependence of the UV-sensitivity $\Delta R/R_0$ for the UV-detector based on single fiber modified by ZnO nanolayer with different thicknesses under 379 nm UV light.

(ZnO layer) was recorded as the response to the UV light, which is an important but simply measurable parameter. We define $\Delta R/R_0$ as the UV-sensitivity, where R_0 refers to the

DOI: 10.1021/acsami.8b04872
ACS Appl. Mater. Interfaces 2018, 10, 23399−23405

original resistance, and ΔR is a time dependent variation of the resistance value ($R-R_0$) under 379 nm UV light. The UV-sensitivity of the single modified fibers detector with different coating thicknesses in composites are shown in Figure 4b. When the UV-light is switched on, the resistance of all the measured detectors decreases with time. When the UV-light is turned off, the resistance can go back to the original value after a long recovery time (see SI Figure S6). It indicates that the single fiber detector can be repeatedly used. Moreover, the slow recovery process is beneficial to the collection of accurate data. Thus, the modified single fiber really presents a potential application as an in situ UV-detector in composites. At the same time, we find the sensitivity shows a sharp thickness dependence. The defined sensitivity of the single fiber detector increases with the decrease of the thickness of ZnO nanolayer. The fiber with 21 nm ZnO nanolayer presents a highest UV-sensitivity.

Additionally, the photoconductive sensitivity is also calculated based on the resistance results as shown in the SI. On the contrary, the single fiber detector with a thinner ZnO nanolayer shows a lower photoconductive sensitivity (see SI Figure S5), because the resistance of the thinner ZnO nanolayer is much higher than that of thicker ZnO nanolayer. However, the calculated photoconductive sensitivity refers to the irradiated surface, which is difficult to accurately measure due to the curved surface of fiber. Therefore, the single ZnO modified fiber can be suggested as a resistive-model sensor in composites to the UV light.

In order to study the performance of the detector of single fiber modified by ZnO under the UV-light the UV-response mechanism of the as-deposited ZnO via ALD is first investigated. The sensitivity, $\Delta R/R_0$, is contributed by three factors as described in the following equation:

$$\Delta R/R_0 = G_1 + G_2 + G_3 \quad (4)$$

where G_1 is the contribution from the improved photocurrent caused by photogenerated electron−hole pairs, G_2 is related to the weakening of the band bending between ZnO and electrode, and G_3 is resultant from the desorption of the adsorbed oxygen ions on the surface of ZnO. Due to the very quick response and short lifetime of photointroduced carriers, the resultant large photocurrents will disappear within a few seconds as the UV light is switched off.[31,32] However, the observed behavior indicates that G_1 is negligible in our case because the recovery process (SI Figure S7) is not as short as expected. In addition, the band effect is rather small in an Ohmic contact (Figure 5b), thus G_2 offers a little bit contribution to the whole sensitivity $\Delta R/R_0$. In this device, therefore, the sensitivity mainly depends on G_3: the adsorption of oxygen on the surface of ZnO nanolayer helps capture free electrons, which leads to the decrease of the conductance. As the electron−hole pairs are generated under the UV light, the holes migrate to the surface that discharges oxygen ions (O_2^-) and desorbs the oxygen. Thus, the conductivity is enhanced and shows a saturation trend.[33,34] While the UV light is turned off, the slow recovery of the resistance (see SI Figure S7) mainly reveals a physisorption process of oxygen that reabsorbs onto the surface and captures the free electrons.[35]

To further reveal the thickness effect on photoelectronic response of the modified fiber, a model is proposed to depict the process with respect to the contribution of G_3. As shown in Figure 5c, a depletion layer is defined in the surface region of ZnO nanolayer, in which the most carriers are trapped by

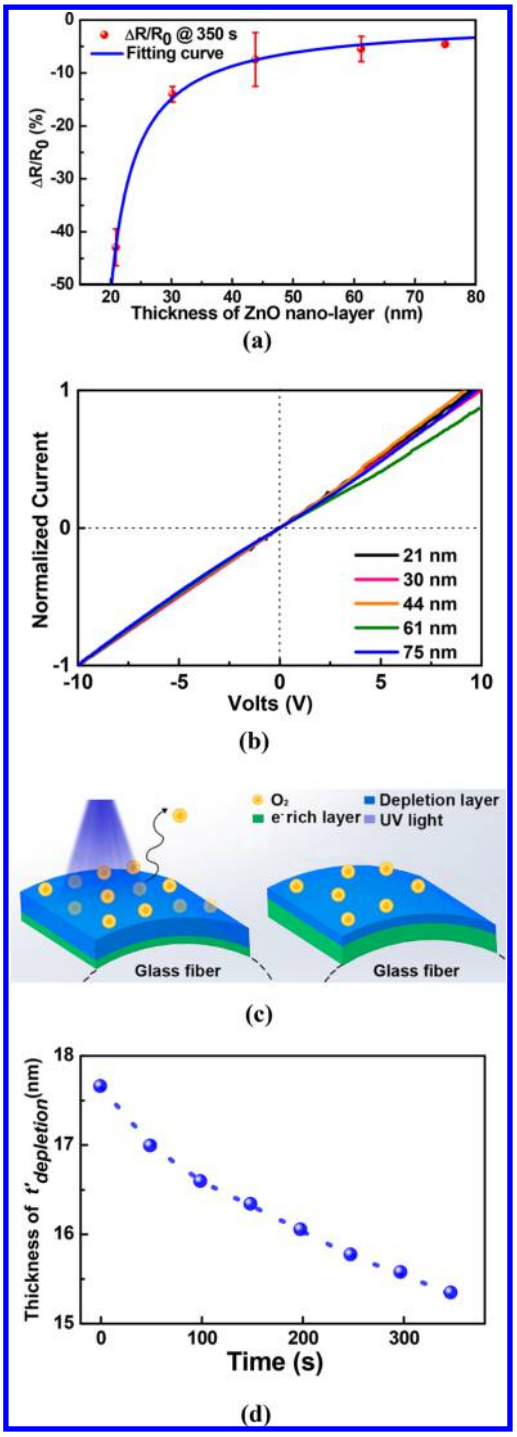

Figure 5. (a) Resistance responses (red symbol) of integrated single fiber device modified by different thicknesses ZnO after exposing to UV light for 350 s. The blue line is the fitting result of the ZnO-thickness dependent UV-sensitivity ($\Delta R/R_0$) with r^2 = 0.999. The error bars represent standard deviations. (b) I−V character of ZnO modified fiber with different thickness. (c) Schematic diagram depicting the O_2^- desorption and carriers-releasing process on the ZnO surface under UV light (left) and the decreased depletion layer after UV irradiation (right). (d) Time dependent on the fitted depletion thicknesses under 379 nm UV-light.

absorbed oxygen. The thickness of the depletion layer is related to the concentration of the adsorbed oxygen ions, which will decrease with time under the UV light. Thus, the complex desorption-adsorption process under the UV light

DOI: 10.1021/acsami.8b04872
ACS Appl. Mater. Interfaces 2018, 10, 23399−23405

may be analyzed through the thickness change of the depletion layer. Then the sensitivity $\Delta R/R_0$ can be calculated as

$$\frac{\Delta R}{R_0} = \frac{S_0}{S} - 1 \tag{5}$$

where S_0 and S are the effective cross section of the ZnO nanolayer before and after UV illumination, respectively. To simplify the model, the initial depletion thickness caused by oxygen adsorption on the surface of ZnO is assumed to be uniform in the same ambient. S_0 and S can be expressed as

$$S_0 = \pi \times ((r_f + t_{ZnO} - t_{depletion})^2 - r_f{}^2) \tag{6}$$

$$S = \pi \times ((r_f + t_{ZnO} - t'_{depletion})^2 - r_f{}^2) \tag{7}$$

where r_f is the radius of glass fiber, t_{ZnO} is the thickness of as-deposited ZnO nanolayer, and $t_{depletion}$ and $t'_{depletion}$ are the thicknesses of the depletion layer before and after UV illumination, respectively.

Therefore, according to the last two equations, eq 5 can be rewritten as

$$\frac{\Delta R}{R_0} = \frac{(r_f + t_{ZnO} - t_{depletion})^2 - r_f{}^2}{(r_f + t_{ZnO} - t'_{depletion})^2 - r_f{}^2} - 1 \tag{8}$$

Least-square fitting of the sensitivity is performed based on the above model. From the experimental data at 350 s, the simulated curve shown in Figure 5a displays a reasonable agreement, which confirms that the relationship between sensitivity $\Delta R/R_0$ and as-deposited ZnO thickness can be analyzed by considering the change of the depletion layer thickness under UV illumination. Meanwhile, the sensitivity of single fiber increases with the decrease of ZnO thickness. However, it need to be emphasized that most of the carriers will be trapped, leading to the restricted mobility of carriers if the as-deposited ZnO thickness is below the fitted initial depletion thickness. In that case, R_0 is so high that the single modified fibers are not suitable for the application as a resistive-model sensor. Thus, the depletion thickness becomes a key factor for designing a high-sensitivity device. To estimate this crucial depletion thickness, we combine the results of $\Delta R/R_0$ of different exposure time (including 50, 100, 150, 200, 250, 300, and 350 s) and fit them simultaneously based on the least-squares method. The fitted thickness of the initial depletion layer is 17.7 nm, which shows a decrease tendency with the increased UV-exposure time as shown in Figure 5d. It means that the deposited thickness of ZnO is required to be very close to the calculated depletion thickness for the purpose of designing a high-sensitivity UV detector. These results reveal that the single fiber coated with ZnO nanolayer can be utilized as an in situ UV detector in composites and its sensitivity can be precisely tuned by modulating the thickness of the nanolayer.

CONCLUSIONS

In summary, the in situ growth of conformal ZnO nanolayer on the surfaces of glass fibers has been achieved by ALD. The thickness of ZnO can be precisely modulated in a single atomic layer scale by varying the number of cycles of ALD, which enables us to investigate the influence of the thickness of modified nanolayer on the macroscopic performance of the composites. The IFSS in the fiber reinforced polymer composites is dramatically enhanced due to the introduction of ZnO nanolayer. Notably, a critical thickness of nanolayer of about 44 nm, is obtained for the first time, giving rise to a maximum relative enhancement of IFSS in the modified fiber composites compared with the control fiber composites. And such enormous enhancement is much higher than the previous reported FRC reinforced by other nanomaterials. The existence of such critical thickness is explained by the change of failure patterns of composites. Furthermore, a potential UV light sensor has been constructed by using a single glass fiber coated with ZnO nanolayer. It is found that the UV-sensitivity is closely related to the thickness of ZnO nanolayer. A theoretical model with the consideration of depletion layer is subsequently proposed to analyze the relationship between thickness of the nanolayer and the UV-sensitivity. In this model, the initial depletion layer thickness before UV illumination is evaluated to be about 17.7 nm, which is a defined parameter to achieve high sensitivity in ZnO-based UV detector. Overall, the results in this work shed light on the long lasting question on how the thickness of nanolayer influences the physical performances of the composites. Based on this work, the new multifunctional composites with higher strength and sensitivity can be designed by controlling the thickness of nanolayer in the interphase region to meet various requirements, so-called the size/thickness engineering.

ASSOCIATED CONTENT

Supporting Information

This material is available free of charge via the Internet The Supporting Information is available free of charge on the ACS Publications website at DOI: 10.1021/acsami.8b04872.

Critical aspect ratios, critical tensile strengths, band gap fitting, photoconductive sensitivity, time dependence of the sensitivity $\Delta R/R_0$ (PDF)

AUTHOR INFORMATION

Corresponding Authors

*(J.Z.) jzhang12@mail.xjtu.edu.cn.
*(W.R.) wren@mail.xjtu.edu.cn.
*(Z.G.Y.) zye@sfu.ca.

ORCID

Jie Zhang: 0000-0003-3472-2274
Yi-Jun Zhang: 0000-0001-8820-2552
Jian Zhuang: 0000-0002-4763-0160
Zuo-Guang Ye: 0000-0003-2378-7304

Notes

The authors declare no competing financial interest.

ACKNOWLEDGMENTS

We acknowledge support from the National Natural Science Foundation of China (No. 51303148), the Fundamental Research Funds for the Central Universities (No. xjj2013018), the National 111 Project of China (B14040) and the Natural Sciences and Engineering Research Council (NSERC) of Canada (Grant No. 203773). The authors also thank X.-F. Gu for help in the fragmentation measurements. We thank the International Center for Dielectric Research (ICDR) for the use of SEM. In addition, we are grateful to Dr. L. Lu for the help in FIB characterization.

DOI: 10.1021/acsami.8b04872
ACS Appl. Mater. Interfaces 2018, 10, 23399−23405

REFERENCES

(1) Mallick, P. K. *Fiber-Reinforced Composites: Materials, Manufacturing, and Design*; CRC press: London, 2007.
(2) Sawpan, M. A.; Pickering, K. L.; Fernyhough, A. Effect of Various Chemical Treatments on the Fiber Structure and Tensile Properties of Industrial Hemp Fibers. *Composites, Part A* **2011**, *42*, 888−895.
(3) Iglesias, J. G.; Gonźalez-Benito, J.; Aznar, A. J.; Bravo, J.; Baselga, J. Effect of Glass Fiber Surface Treatments on Mechanical Strength of Epoxy Based Composite Materials. *J. Colloid Interface Sci.* **2002**, *250*, 251−260.
(4) Meng, F.; Zhao, J.; Ye, Y.; Zhang, X.; Li, Q. Carbon nanotube fibers for electrochemical applications: effect of enhanced interfaces by an acid treatment. *Nanoscale* **2012**, *4*, 7464−7468.
(5) Dai, Z.; Zhang, B.; Shi, F.; Li, M.; Zhang, Z.; Gu, Y. Effect of Heat Treatment on Carbon Fiber Surface Properties and Fibers/Epoxy Interfacial Adhesion. *Appl. Surf. Sci.* **2011**, *257*, 8457−8461.
(6) Wu, G. M. Oxygen Plasma Treatment of High Performance Fibers for Composites. *Mater. Chem. Phys.* **2004**, *85*, 81−87.
(7) Sager, R. J.; Klein, P. J.; Lagoudas, D. C.; Zhang, Q.; Liu, J.; Dai, L. Effect of Carbon Nanotubes on the Interfacial Shear Strength of T650 Carbon Fiber in An Epoxy Matrix. *Compos. Sci. Technol.* **2009**, *69*, 898−904.
(8) Zhang, J.; Zhuang, R.; Liu, J.; Mäder, E.; Heinrich, G.; Gao, S. Functional Interphases with Multi-Walled Carbon Nanotubes in Glass Fiber/Epoxy Composites. *Carbon* **2010**, *48*, 2273−2281.
(9) Luo, H.; Xiong, G.; Chen, X.; Li, Q.; Ma, C.; Li, D.; Wu, X.; Wan, Y. ZnO Nanostructures Grown on Carbon Fibers: Morphology Control and Microwave Absorption Properties. *J. Alloys Compd.* **2014**, *593*, 7−15.
(10) Lin, Y.; Ehlert, G.; Sodano, H. A. Increased Interface Strength in Carbon Fiber Composites Through a ZnO Nanowire Interphase. *Adv. Funct. Mater.* **2009**, *19*, 2654−2660.
(11) Ehlert, G. J.; Sodano, H. A. Zinc Oxide Nanowire Interphase for Enhanced Interfacial Strength in Lightweight Polymer Fiber Composites. *ACS Appl. Mater. Interfaces* **2009**, *1*, 1827−1833.
(12) Ehlert, G. J.; Lin, Y.; Galan, U.; Sodano, H. A. Interaction of ZnO Nanowires with Carbon Fibers for Hierarchical Composites with High Interfacial Strength. *J. Solid Mech. Mater. Eng.* **2010**, *4*, 1687−1698.
(13) Galan, U.; Lin, Y.; Ehlert, G. J.; Sodano, H. A. Effect of ZnO Nanowire Morphology on the Interfacial Strength of Nanowire Coated Carbon Fibers. *Compos. Sci. Technol.* **2011**, *71*, 946−954.
(14) Gao, S.; Zhuang, R. C.; Zhang, J.; Liu, J. W.; Mäder, E. Glass Fibers with Carbon nanotube Networks as Multifunctional Sensors. *Adv. Funct. Mater.* **2010**, *20*, 1885−1893.
(15) Rausch, J.; Mäder, E. Health Monitoring in Continuous Glass Fiber Reinforced Thermoplastics: Manufacturing and Application of Interphase Sensors Based on Carbon Nanotubes. *Compos. Sci. Technol.* **2010**, *70*, 1589−1596.
(16) Liao, Q.; Mohr, M.; Zhang, X.; Zhang, Z.; Zhang, Y.; Fecht, H. J. Carbon Fiber−ZnO Nanowire Hybrid Structures for Flexible and Adaptable Strain Sensors. *Nanoscale* **2013**, *5*, 12350−12355.
(17) Wang, Z. L. Zinc Oxide Nanostructures: Growth, Properties and Applications. *J. Phys.: Condens. Matter* **2004**, *16*, R829.
(18) Son, D. I.; Kwon, B. W.; Park, D. H.; Seo, W. S.; Yi, Y.; Angadi, B.; Lee, C.; Choi, W. K. Emissive ZnO-Graphene Quantum Dots For White-Light-Emitting Diodes. *Nat. Nanotechnol.* **2012**, *7*, 465−471.
(19) Jur, J.; Sweet, W. J.; Oldham, C. J.; Parsons, G. N. Atomic Layer Deposition of Conductive Coatings on Cotton, Paper, and Synthetic Fibers: Conductivity Analysis and Functional Chemical Sensing Using "All-Fiber"Capacitors. *Adv. Funct. Mater.* **2011**, *21*, 1993−2002.
(20) George, S. M. Atomic Layer Deposition: An Overview. *Chem. Rev.* **2009**, *110*, 111−131.
(21) Kelly, A.; Tyson, W. R. Tensile Properties of Fiber-Reinforced Metals: Copper/Tungsten and Copper/Molybdenum. *J. Mech. Phys. Solids* **1965**, *13*, 329−350.
(22) Wimolkiatisak, A. S.; Bell, J. P. Interfacial Shear Strength and Failure Modes of Interphase-Modified Graphite-Epoxy Composites. *Polym. Compos.* **1989**, *10*, 162−172.
(23) Godara, A.; Gorbatikh, L.; Kalinka, G.; Warrier, A.; Rochez, O.; Mezzo, L.; Luizi, F.; Vuure, A.W. van; Lomov, S. V.; Verpoest, I. Interfacial Shear Strength of A Glass Fiber/Epoxy Bonding in Composites Modified with Carbon Nanotubes. *Compos. Sci. Technol.* **2010**, *70*, 1346−1352.
(24) Gao, S.; Mäder, E.; Plonka, R. Nanocomposite Coatings for Healing Surface Defects of Glass Fibers and Improving Interfacial Adhesion. *Compos. Sci. Technol.* **2008**, *68*, 2892−2901.
(25) Galiotis, C.; Young, R. J.; Yeung, P. H. J.; Batchelder, D. N. The Study of Model Polydiacetylene/Epoxy Composites. *J. Mater. Sci.* **1984**, *19*, 3640−3648.
(26) Asloun, E. I. M.; Nardin, M.; Schultz, J. Stress Transfer in Single-Fiber Composites: Effect of Adhesion, Elastic Modulus of Fiber and Matrix, and Polymer Chain Mobility. *J. Mater. Sci.* **1989**, *24*, 1835−1844.
(27) Fang, T. H.; Chang, W. J.; Lin, C. M. Nanoindentation Characterization of ZnO Thin Films. *Mater. Sci. Eng., A* **2007**, *452*, 715−720.
(28) Yen, C. Y.; Jian, S. R.; Chen, G. J.; Lin, C. M.; Lee, H. Y.; Ke, W. C.; Liao, Y. Y.; Yang, P. F.; Wang, C. T.; Lai, Y. S.; Jang; Jason, S. C.; Juang, J. Y. Influence of Annealing Temperature on the Structural, Optical and Mechanical Properties of ALD-Derived ZnO Thin Films. *Appl. Surf. Sci.* **2011**, *257*, 7900−7905.
(29) Wong, C. P.; Bollampally, R. S. Thermal Conductivity, Elastic Modulus, and Coefficient of Thermal Expansion of Polymer Composites Filled with Ceramic Particles for Electronic Packaging. *J. Appl. Polym. Sci.* **1999**, *74*, 3396−3403.
(30) Hsueh, C. H. Analytical Evaluation of Interfacial Shear Strength for Fiber-Reinforced Ceramic Composites. *J. Am. Ceram. Soc.* **1988**, *71*, 490−493.
(31) Boix, P. P.; Ajuria, J.; Pacios, R.; Garcia-Belmonte, G. Carrier Recombination Losses in Inverted Polymer: Fullerene Solar Cells with ZnO Hole-Blocking Layer From Transient Photovoltage and Impedance Spectroscopy Techniques. *J. Appl. Phys.* **2011**, *109*, 074514.
(32) Liu, Y.; Gorla, C. R.; Liang, S.; Emanetoglu, N.; Lu, Y.; Shen, H.; Wraback, M. Ultraviolet Detectors Based on Epitaxial ZnO Films Grown by MOCVD. *J. Electron. Mater.* **2000**, *29*, 69−74.
(33) Liu, M.; Kim, H. K. Ultraviolet Detection with Ultrathin ZnO Epitaxial Films Treated with Oxygen Plasma. *Appl. Phys. Lett.* **2004**, *84*, 173−175.
(34) Jin, Y.; Wang, J.; Sun, B.; Blakesley, J. C.; Greenham, N. C. Solution-Processed Ultraviolet Photodetectors Based on Colloidal ZnO Nanoparticles. *Nano Lett.* **2008**, *8*, 1649−1653.
(35) Li, Q. H.; Gao, T.; Wang, Y. G.; Wang, T. H. Adsorption and Desorption of Oxygen Probed from ZnO Nanowire Films by Photocurrent Measurements. *Appl. Phys. Lett.* **2005**, *86*, 123117.

DOI: 10.1021/acsami.8b04872
ACS Appl. Mater. Interfaces 2018, 10, 23399−23405